DEUTSCHES ELEKTRONEN – SYNCHROTRON

DESY 93–014
February 1993

First Measurements at HERA of Deep Inelastic Scattering at Low x

A. De Roeck

Deutsches Elektronen-Synchrotron DESY, Hamburg

M. Klein

Deutsches Elektronen-Synchrotron DESY
Institut für Hochenergiephysik IfH, Zeuthen

ISSN 0418-9833

NOTKESTRASSE 85 · D-2000 HAMBURG 52

To be sure that your preprints are promptly included in the
HIGH ENERGY PHYSICS INDEX,
send them to (if possible by air mail):

DESY **Bibliothek** **Notkestraße 85** **W-2000 Hamburg 52** **Germany**	**DESY-IfH** **Bibliothek** **Platanenallee 6** **O-1615 Zeuthen** **Germany**

DESY 93-014
February 1993

ISSN 0418-9833

FIRST MEASUREMENTS AT HERA OF DEEP INELASTIC SCATTERING AT LOW x*

Albert De Roeck
Deutsches Elektronen Synchrotron
D-2000 Hamburg 52, Notkestrasse 85, Germany

and

Max Klein
Deutsches Elektronen Synchrotron, Institut für Hochenergiephysik
D-O 1615 Zeuthen, Platanenallee 6, Germany

ABSTRACT

In 1992 HERA, the first electron-proton colliding accelerator, came into operation. This paper presents a brief account on HERA's history, components and performance. The methods of both HERA experiments, H1 and ZEUS, are explained which lead to the identification of about 100 deep inelastic events among a huge background caused mainly by proton beam interactions and photoproduction events. The published results of the two experiments are compared, based on the the first data obtained in summer 1992 with an integrated luminosity of about 2 nb^{-1}. The phenomenology and HERA perspectives of deep inelastic physics at low x are discussed.

1. Introduction

The 1992 San Miniato conference gave us the possibility for the first international announcement of the successful observation of deep inelastic electron proton interactions at HERA. Fig. 1 shows an event which was taken the day before the conference began. It represented evidence for deep inelastic scattering observed in the H1 detector, a similar interaction having been observed in the ZEUS apparatus. A cluster of a few GeV energy had been measured in the H1 backward electromagnetic calorimeter in coincidence with a signal of the adjacent backward proportional chamber. The observed event has a momentum transfer squared of Q^2 = 18 GeV^2 and an x value of 0.0004. A new chapter of the physics of deep inelastic scattering had been opened after the evidence for quarks in the sixties [1] and the detailed exploration of quark-gluon interactions in the muon and neutrino fixed target experiments of the seventies and eighties.

This report has been written about half a year after the conference [2] and thus cannot simply reflect the contents of our talks on "HERA" and on "Low x Physics". Meanwhile we had the privilege to participate in the data taking, analysis and publication of the first deep inelastic cross section measurements at HERA which, in agreement with the organizers, we have chosen to describe, together with an account of the HERA machine and the phenomenology of the physics at low

*Invited Talks presented at the International Conference on the Standard Model and Just Beyond, San Miniato, Italy, June 1992

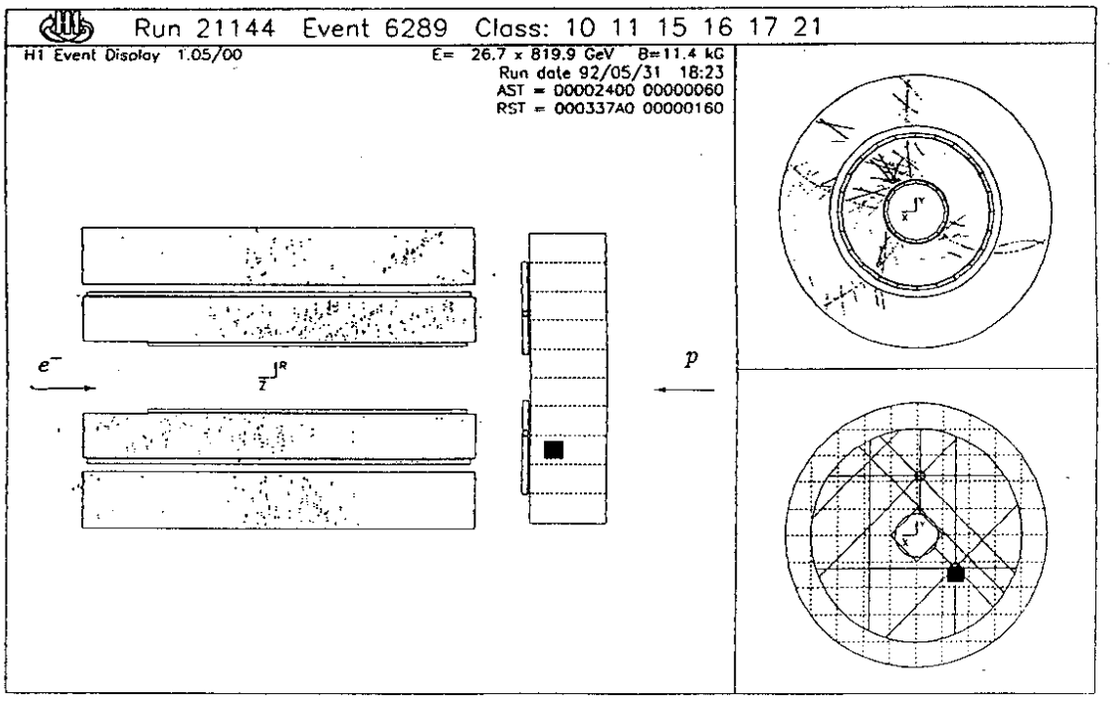

Figure 1: *Deep inelastic event candidate observed in the H1 detector on May 31, 1992, the first day of HERA's operation*

x. HERA explores the region of high parton densities where standard perturbative Quantum Chromodynamics may not be sufficient anymore to describe the evolution of the proton structure functions. Exciting measurements are to be made in the near future.

The paper has 5 sections describing the HERA accelerator complex, the experiments and kinematics, the refined methods to identify deep inelastic reactions within a huge "background" of beam interaction events, explaining the cross section measurements and finally presenting an experimentalists view on the physics at low x to be explored at HERA.

2. HERA

About 15 years ago several proposals were circulating for electron-proton colliders at DESY, CERN and Fermilab. These appeared to be the obvious possibility for extending the centre of mass energy s, i.e. the maximum momentum transfer squared Q^2, from $s = 2 \cdot M_p \cdot E_l \leq 1000\ GeV^2$ for the ongoing fixed target lepton-proton experiments to $s = 4 \cdot E_e \cdot E_p \leq 10^5 GeV^2$ at HERA. In July 1981 the construction of the Hadron-Elektron-Ring-Anlage (HERA) was proposed to collide 10-30 GeV electrons or positrons off 300-820 GeV protons with a luminosity above $10^{31} cm^{-2} s^{-1}$. Ten years after, in October 1991, the first interactions of 12 GeV electrons and 480 GeV protons were observed at DESY. Last year data were taken, analyzed and published

which belong to a so far unaccessed kinematic region. Milestones of the HERA development are summarized in Table 1.

date	achievement
July 1981	HERA proposal $E_e = 10 - 30\ GeV$, $E_p = 300 - 820\ GeV$
April 1984	approval of HERA with 654 MDM (15% from abroad)
July 1986	recommendation by the PRC to approve H1 and ZEUS
November 1986	end of PETRA e^+e^- runs
August 1987	tunnel drilled, "arrival of HERAKLES"
August 1988	electrons in HERA
April 1990	first proton ring octant cold
November 1990	last superconducting dipole installed, "HERA complete"
April 1991	protons injected and stored
June 1991	superconducting cavities for e beam, 30 GeV reached
October 1991	first collision: 12 and 26 GeV x 480 GeV, $L \sim 10^{27} cm^{-2} s^{-1}$
during 1991	cosmic runs of the detectors
31.5.1992	first HERA collisions, beginning of HERA physics
September 1992	observation of 60% transverse electron polarization
October 1992	PRC recommendation to approve HERMES

Table 1: *Milestones for the completion of HERA*

In order to inject electrons and protons into the HERA ring, various **preaccelerators** had to be built or/and reconstructed: three LINAC's of 20, 70 and 32 m length for the acceleration of e^- (I), e^+ (II) and negative hydrogen atoms (III) to energies of 220, 450 and 50 MeV, respectively; in 1986 the electron synchrotron DESY II replaced the old DESY I acting as the injector of 7 GeV electrons into the PETRA ring where the electrons are accelerated to maximum 14 GeV. A new proton synchrotron (DESY III) of 317 m diameter was constructed to reach 7.5 GeV energy prior to injection into PETRA which in turn provides 40 GeV proton injection energy. An overview over the accelerator system is given in Fig. 2.

HERA is an accelerator with warm and with superconducting magnets and cavities. The **proton ring** consists of 104 cells of superconducting magnets (4 dipoles, 2 quadrupoles and correction magnets, 47 m long each cell) for bend and focus. One of the straight sections contains warm cavities, a 52 MHz system accelerating bunches of 1.15 m length at an RF voltage of 280 kV and a 208 MHz cavity system leading to a bunch length of 0.27 m at 820 GeV proton energy. The extension of the interaction region over a few tens of cm has been an important feature of triggering and analyzing ep interactions. During the development and construction phase several important changes were made of the dipole concept as the increase of the magnet length, the choice of a cold iron yoke surrounding the collared coil instead of a yoke outside the coil cryostat and the introduction of deca-(dodeca) pole correction windings on the dipoles (quadrupoles). That happened in 1988 only when the possible perturbation of the low field during injection which results from

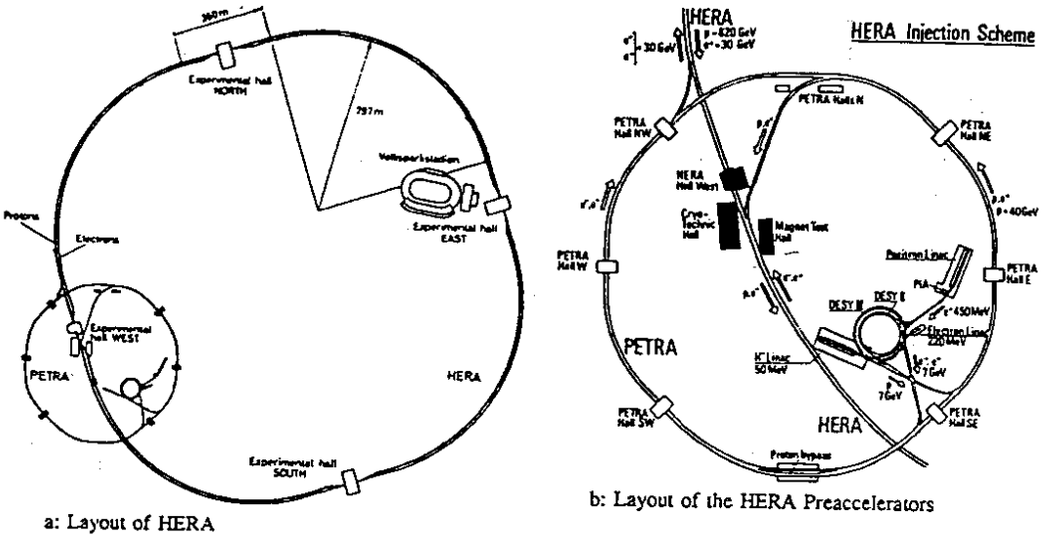

a: Layout of HERA

b: Layout of the HERA Preaccelerators

Figure 2: *The accelerator complex at DESY, Hamburg*

eddy currents in the superconductor became a major concern. More than 1000 km of superconducting cables were needed, each cable containing 24 wires made of 1230 NbTi filaments of 12 μm diameter.

The **electron ring** consists of 416 warm magnet modules (1 dipole, 1 quad, 2 sextupoles, 12 m long each module). Acceleration is achieved by 82 warm cavities (from PETRA) which are designed to run at about 27 GeV with 60 mA current. The HERA design energy can be reached utilizing the 16 superconducting cavities providing a gradient of about 5 MV/m which gives about 3 GeV more electron energy at the same currents. Synchrotron radiation leads to transverse electron polarization [3] of at most $\lambda = 8/5\sqrt{3}$. An impressive series of measurements, though not in colliding mode and with the detector solenoids switched off, lead to a reproducible measurement of $\lambda \leq 0.60$ [4]. The apparent understanding of the resonance conditions between the spin revolution and the betatron frequency will possibly allow to tune the polarization to certain values which are of interest for future studies of electroweak cross sections as the search for right handed weak charged currents. During the shutdown 1993/94 it is foreseen to install spin rotating magnets [5] in order to turn the transverse into longitudinal polarization.

Operation of HERA for physics began in May 1992. Fig. 3 illustrates the life times of electron and proton fillings which determine the way to run the detectors. Every 2-3 hours the sense wire voltage of the tracking detectors near the beam pipe had to be switched off in order to allow for a new electron filling. Usually 2 electron fills were made until both e and p had to be refilled, the proton lifetime depending on the number of bunches in the ring. HERA is designed [6] to contain 210 e and p bunches. Of particular use for background and timing studies have been the e (p) pilot bunches which have no counterpart in the p (e) ring. For data taking and analysis, HERA is a very complicated environment as it combines the disadvantages of e^+e^- machines (large synchrotron radiation and electroweak cross sections) and

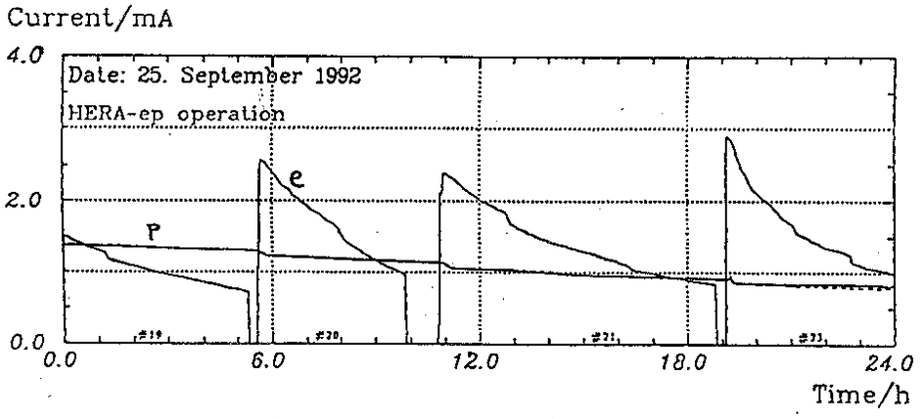

Figure 3: *Electron and proton bunch intensity versus time. In September 1992 HERA ran in 10 bunch mode.*

proton rings (strong interaction backgrounds due to proton restgas and beam wall scattering). The deep inelastic signal to beam background ratio is of the order of 10^{-4}, the bunch crossing frequency 10.4 MHz.

In 1992 most of the data were taken with 10 bunches. Table 2 compares some of the relevant characteristics for 1992 with their design values. In the fall

parameter	typical value in 1992	design value
E_p	820 GeV	820 GeV
E_e	26.7 GeV	30 GeV
nr of bunches	10	210
p current/bunch	0.2 mA	0.75 mA
e current/bunch	0.2 mA	0.26 mA
max. luminosity	$3 \cdot 10^{29} cm^{-2} s^{-1}$	$1.5 \cdot 10^{31} cm^{-2} s^{-1}$
$\int_{year} lumi$	30 nb^{-1}	50 pb^{-1}

Table 2: *Comparison of some HERA parameters reached in the first few months of running in collider mode with their design values.*

1992, after the end of data taking, several improvements were made. The electron beam was operated with 110 bunches with a total current of up to 23 mA. The proton ring stored 160 bunches which gave 13 mA. It is therefore likely that the integrated luminosity can be increased further, from about 2 nb^{-1} in the summer 1992, and 30 nb^{-1} in the fall to perhaps 1 or 10 pb^{-1} in 1993 which would allow to

access the high Q^2 region with interesting rates.

3. Detectors and Kinematics

Two experiments, H1 and ZEUS [7,8], recorded ep collisions at HERA in summer 1992. Both experiments have tracker, calorimeter and muon detectors and an electron tagger system. The calorimeter is an important component in the design of both detectors. The H1 collaboration has opted for liquid argon calorimetry, which is well taylored to identify and measure electrons. The large granularity of this calorimeter is exploited to compensate the intrinsically different e/π response by software weighting algorithms. In the backward region H1 has an electromagnetic calorimeter which is made of lead/scintillator stacks. ZEUS has chosen to emphasize on the quality of the hadron measurement by constructing an inherently compensating uranium/scintillator calorimeter. The expected resolutions for both experiments are (energy in GeV):

$$\text{H1}: \quad \frac{\Delta E_{\text{em}}}{E} = \frac{0.10}{\sqrt{E}} \oplus 0.02 \; ; \quad \frac{\Delta E_{\text{had}}}{E} = \frac{0.50}{\sqrt{E}} \oplus 0.02 \tag{1}$$

$$\text{ZEUS}: \quad \frac{\Delta E_{\text{em}}}{E} = \frac{0.18}{\sqrt{E}} \oplus 0.01; \quad \frac{\Delta E_{\text{had}}}{E} = \frac{0.35}{\sqrt{E}} \oplus 0.01 \tag{2}$$

Detecting charged particles from the interaction region has shown to be of invaluable importance for understanding the first HERA data. Both experiments have tracking detectors, consisting of several modules of drift and proportional chambers. For the 1992 data taking period the ZEUS central tracking was only partially equipped with readout electronics.

At HERA the luminosity is measured *via* the elastic bremsstrahlung reaction $ep \rightarrow ep\gamma$ which, according to the Bethe-Heitler [9] cross section formula, depends on the secondary energies E_e' and E_γ only. Both experiments have installed luminosity monitor systems to measure both energies with an electron tagger for very small angle scattering at about -30m downstream the electron beam and a photon detector at $z \sim -100m$. These detectors are electromagnetic calorimeters using TlCl/TlBr crystals for H1 [10] and a Pb/SCSN38 scintillator sandwich for ZEUS [11]. The integrated luminosity measurement for the first published deep inelastic cross sections was quoted to be accurate to 7 (14) % for H1 (ZEUS) [12,13].

The kinematics of the inclusive neutral-current reaction $ep \rightarrow eX$ at fixed centre of mass energy s is determined by two variables usually taken as x, the Bjorken scaling variable and Q^2, the negative four-momentum transfer squared from the electron to the proton. According to $Q^2 = sxy$ both are related *via* the relative energy transfer y. Contrary to some fixed target lepton-hadron scattering experiments of the past, the HERA experiments simultaneously measure the scattered electron and reconstruct the hadronic final state, i.e. the energies E_e' and E_h and the angles θ_e and θ_h. The polar angles are measured relatively to the proton beam direction. The

hadronic polar angle can be measured utilizing

$$cos\theta_h = \frac{(\sum_h p_x)^2 + (\sum_h p_y)^2 - (\sum_h (E - p_z))^2}{(\sum_h p_x)^2 + (\sum_h p_y)^2 + (\sum_h (E - p_z))^2} \tag{3}$$

which relates *via* four-momentum conservation θ_h to the hadronic energy flow. The measurement of the two angles θ_e and θ_h can be used to replace the direct measurement of the secondary electron energy by a measurement of the electron angle and of the hadron momenta and energies [14] according to

$$E_e' = E_e \cdot \frac{2sin\theta_h}{sin\theta_h + sin\theta_e - sin(\theta_e + \theta_h)}. \tag{4}$$

At the tree level all combinations of two of these variables are equivalent and may be chosen to determine Q^2 and x. Depending on the kinematic region and on experimental preferences (resolution, calibration) different choices have been made by the two experiments which are listed in Table 3. The y variable can be calculated directly from the electron or according to [15] from the hadrons

$$y_e = 1 - E_e'/E_e \cdot sin^2\theta_e/2 \qquad y_h = \sum_h (E - p_z)/2E_e. \tag{5}$$

H1 switched from y_e to y_h at lower y because the resolution $\delta x/x$ of $x = Q_e^2/sy_e$ diverges like $1/y$ at low y. The choice of variables affects the amount of radiative corrections which, for example, chosing Q_e^2, y_e are large ($\sim 30\%$) at low x but much smaller if y_e is replaced by y_h [16].

experiment	Q^2	y
H1	$4E_eE_e'cos^2\theta_e/2$	y_e for $y_e > 0.1$ y_h for $y_e < 0.1$
ZEUS	$4E_eE(\theta_e, \theta_h) \cdot cos^2\theta_e/2$	$y(\theta_e, \theta_h)$

Table 3: *Choices of H1 and ZEUS to determine the variables Q^2 and $x = Q^2/sy$ in their first publications on deep inelastic scattering.*

Fig. 4 displays isoangle and isoenergy lines in the kinematic Q^2, x plane focussing on the region of the first HERA measurements. Due to the very large c.m.s. energy very small x values become accessible for the first time. A typical event at $Q^2 \sim 10\ GeV^2$ and $x \sim 10^{-3}$ is characterized by an electron scattered into the backward region at $\theta_e \sim 170°$, relatively to the proton beam direction, and an energy E_e' of about 20 *GeV*. The accompanying hadronic system has an average angle of about 120° and about 8 *GeV* energy. At extremely low x the average θ_h is about 170°, i.e. both the electron and the hadronic system, on average, are scattered backwards.

4. Observation of Deep Inelastic Scattering Events

The first deep inelastic scattering (DIS) analyses at HERA are based upon a total integrated luminosity of $(1.3 \pm 0.1) nb^{-1}$ and of $(2.1 \pm 0.3) nb^{-1}$ for H1 and ZEUS,

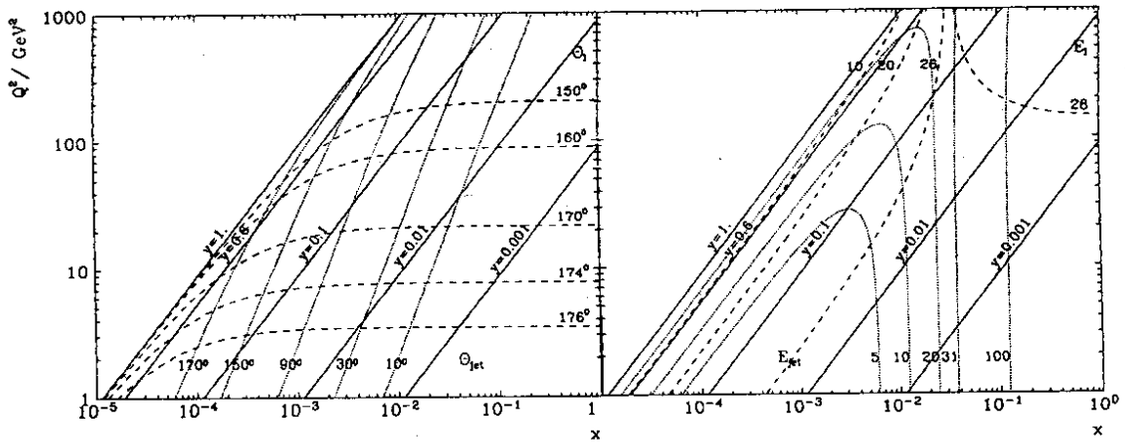

Figure 4: *Lines of constant scattering angles and energies in the Q^2, x plane at HERA for $E_e = 26.7$ GeV and $E_p = 820$ GeV.*

respectively. In the Born approximation the deep inelastic scattering cross section at low Q^2 is determined by the two structure functions F_2 and $2xF_1 = F_2/(1+R)$:

$$\frac{d^2\sigma}{dxdQ^2} = \frac{2\pi\alpha^2}{Q^4 x}(2\ (1-y)\ +\ \frac{y^2}{1+R})F_2(x,Q^2). \tag{6}$$

Due to the $1/Q^4$ dependence of the cross section most of the DIS events are concentrated at low Q^2 values. In fact, for the presently analysed data samples only a few events with $Q^2 > 100$ GeV^2 are expected. For low values of Q^2 the scattered electron deposits its energy in the backward calorimeter, see Fig. 4. Typical DIS event candidates detected in the H1 and ZEUS detectors are shown in Fig. 5. For H1 the scattering angle is determined from the reconstructed space point in a backward planar proportional chamber and the reconstructed event vertex. At smaller θ_e, the electron track is reconstructed in the central tracking chambers. The angular resolution is about 6 *mrad*. ZEUS reconstructs the electron position in the calorimeter using the energy sharing between photomultipliers and calorimeter cells. The obtained angular resolution amounts to 10 *mrad*.

At HERA the electroweak interaction rate is several orders of magnitude smaller than the background rate caused by strong interactions of beam protons with either the residual gas in the beampipe or with the material of the beampipe itself. Moreover, at low scattered electron energies, the background rate due to photoproduction events is much larger than the rate of deep inelastic events. One of the important issues of the first analyses was to show that DIS events can be isolated from the background reactions. More details on the experimental procedures are given in [12,13].

Both experiments use a trigger based on a minimal energy requirement of a few *GeV* in a calorimeter trigger tower and on timing information. The ZEUS experiment exploits the fast time resolution of the calorimeter response of energetic signals (~ 1 *ns* for DIS events) to reject interactions which originate from outside

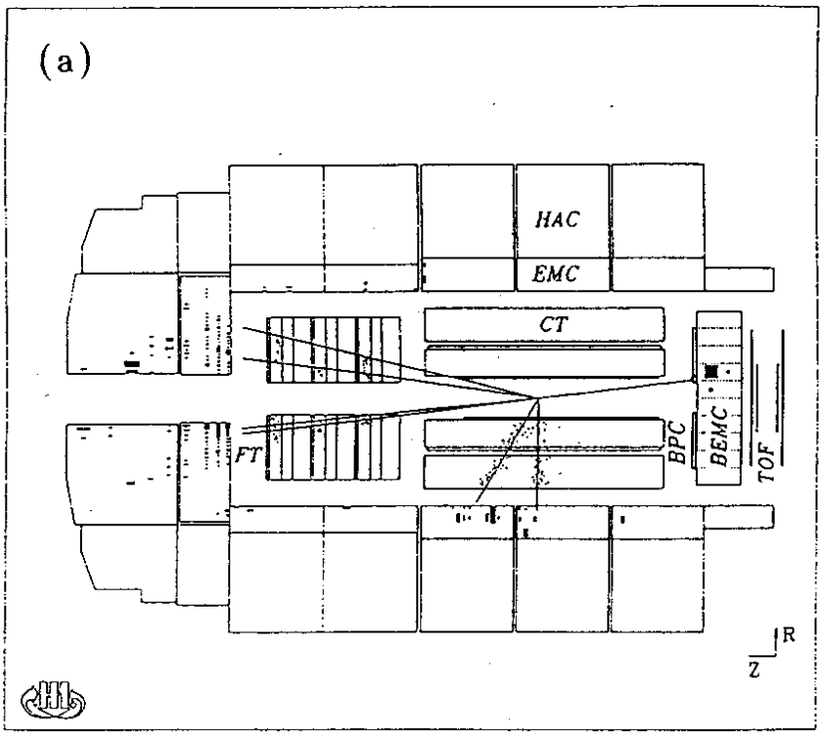

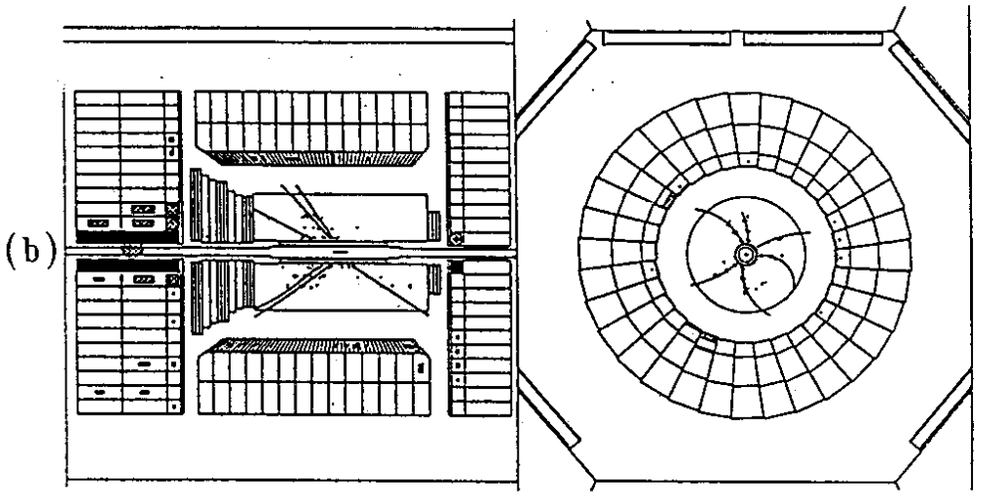

Figure 5: *DIS event candidates as seen in the H1 (a) and ZEUS (b) experiment. The kinematic values are* $Q^2 = 17\ GeV^2$ *and* $x = 0.002$ *for H1 and* $Q^2 = 6\ GeV^2$ *and* $x = 0.0004$ *for ZEUS.*

the detector. H1 has shielded for this purpose the proton side of the experiment with time of flight scintillation counters. The ZEUS (H1) experiment recorded in total about 10^6 ($6 \cdot 10^4$) triggers for DIS event candidates, several orders of magnitude larger than the expected number of produced deep inelastic scattering events.

ZEUS sharpens the trigger energy and timing requirements offline to select DIS event candidates. An electromagnetic energy cluster with energy larger than 2.5 ... 5 GeV is required to be present. The H1 offline event selection requires an energy cluster of at least 4 GeV accompanied by a reconstructed space point in the backward proportional chamber, and, for cluster energies below 22 GeV, at least one track in the central tracker ($20^0 < \theta < 160^0$).

For both experiments the final challenge is to purify the sample from ep photoproduction background, which manifests itself at low scattered electron energies (high y region). These events are produced copiously: the measured ep photoproduction cross section for $E_\gamma > 1$ GeV is of the order of 20 μb at HERA energies, i.e. about hundred times larger than the DIS cross section for $Q^2 > 5$ GeV^2. For photoproduction events the scattered electron remains in the beampipe and will generally not be detected by the electron tagger. The particles produced in photoproduction events can mimic a scattered electron in the H1 and ZEUS detector through pion-photon overlap or converted photons. The two experiments used similar techniques to suppress this background. ZEUS relies on the quantity

$$\delta = \sum_i (E - p_Z)_i = 2E_e \cdot (1 - y_e + y_h) \tag{7}$$

where i extends over all calorimeter cells above some threshold. This variable minimizes the effect of proton remnant particles in the beampipe, for which $E \simeq p_Z$, and equals $\delta \simeq 2E_e$ if all particles are detected. Photoproduction events are located at smaller δ values as a result of the escaping scattered electron and hadrons in the backward region. Events are selected as DIS candidates if $35GeV < \delta < 60GeV$. In the H1 analysis the values of y_e and y_h are compared, which should be identical within resolution for non-radiative DIS events. For y_e values smaller than 0.6, events are removed if $y_h < y_e/2$. The region around the beam pipe was excluded demanding the electromagnetic cluster position to be outside a box of 32x32 cm^2. Both experiments have succeeded in keeping the total beam induced background and the photoproduction contamination in the final DIS candidate sample used for cross section measurements below 10%.

The scattered electron energy distributions from the resulting event samples are presented in Fig. 6. As expected from the shape of the electron isoenergy lines in the Q^2, x plane, Fig. 4, the distributions show a clear peak near the value of the electron beam energy. The H1 spectrum is calculated from energy measurements in the backward calorimeter, while the ZEUS spectrum is derived from the electron and hadronic polar angles. The Monte Carlo spectra rely on events generated using HERACLES [17] for the electroweak interaction, which includes first order radiative corrections, followed by LEPTO 5.2 [18] (H1) or ARIADNE [19] (ZEUS) for the simulation of QCD processes. The parton distributions were chosen to

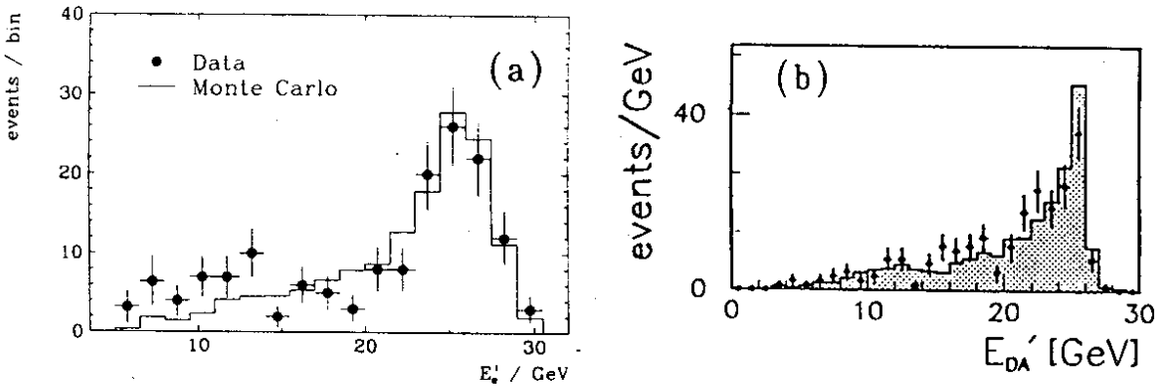

Figure 6: *The scattered electron energy distribution for a) H1 : electron energy measured in the calorimeter b) ZEUS : electron energy determined from θ_e and θ_h.*

be the MRSD0 parametrization described in [20]. The peak position, shape and normalization of the energy distributions are well described by the Monte Carlo calculations which include a full simulation of the detector.

5. Cross Section Measurements of H1 and ZEUS

Very recently both experiments have published their first inclusive deep inelastic scattering cross section measurements. Fig. 7 shows the distribution of events registered by the experiments in the Q^2, x plane. The variables were calculated as summarized in Table 3. In view of the very limited statistics of the first data about 5

experiment	lumi	events	Q^2_{min}	x_{min}	y_{min}	y_{max}	$E'_{e,min}$	$\theta_{e,min}$
H1	1.3 nb^{-1}	72	5	10^{-4}	0.025	0.6	-	174°
ZEUS	2.1 nb^{-1}	117	10	$5 \cdot 10^{-4}$	0.020	-	5 *GeV*	-

Table 4: *Luminosity, rate and effective cuts for cross section analyses of both HERA experiments.*

significant bins were chosen, H1 presenting projections of the cross section *versus* Q^2 and $log_{10}(x)$ and ZEUS a double differential measurement in coarse $log_{10}(Q^2), log_{10}(x)$ bins. The measured cross sections are shown in Fig. 8. The Q^2 and x resolutions for H1 [12] and ZEUS [21] are summarized in Table 5. Up to about 40% corrections were applied for acceptance and smearing effects. The radiative corrections to the Born cross section depend on the choice of variables. H1 did not apply the radiative corrections while ZEUS did. This leads to an additional error of the ZEUS result of up to 20% since the corrections, mainly due to the Born cross section itself [22],

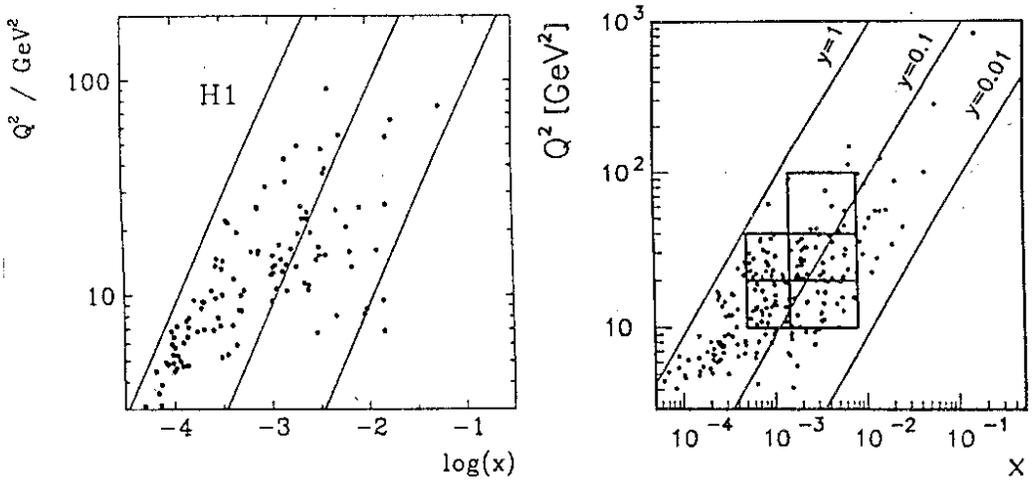

Figure 7: *Scatter plot of the event population for H1 and ZEUS. Additional cuts were made as listed in Table 4, i.e. only a subsample of the events shown here was used to calculate the cross sections.*

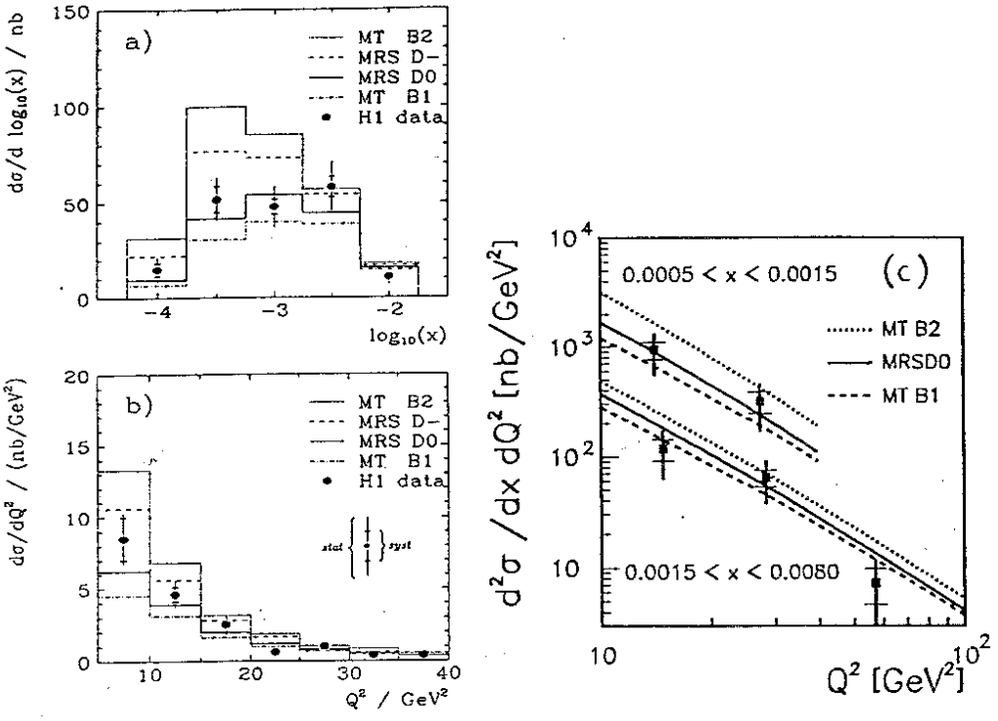

Figure 8: *Cross section measurement of H1 (a,b) and ZEUS (c)*

experiment	$\delta Q^2/Q^2$	$\delta x/x$
H1	6% rather constant	15% at 10^{-4}, 35% at 10^{-2}
ZEUS	12% at 10, 18% at 100 GeV^2	45% at $5 \cdot 10^{-4}$, 30% at 10^{-2}

Table 5: *Resolutions of Q^2 and x. The differences reflect not only the different apparatus but also the ways to calculate the secondary electron energy.*

can depend largely on the structure function chosen. The limited amount of data prevents an iterative procedure to reduce the structure function dependence to the per cent level. Apart from the radiative corrections the dominating systematic uncertainty of the ZEUS measurement is given by an error of 14% common to all points due to the luminosity measurement uncertainty. The systematic error of the H1 measurement is dominated, at lowest Q^2 and x, by the residual photoproduction background (+15% for the lowest x and Q^2 bin). Various error sources like possible shifts of the electron energy and theta measurement add up to an average systematic error for H1 of about 11%, apart from the lowest bins which have an error of about 25%. All points have in common a 7% luminosity error which has not been added to the systematic error bars.

In Fig. 8 a comparison is made with cross section calculations based on various parton distribution parametrizations which differ in the assumptions on the behaviour of quark and gluon densities at low x [20,23]. The MTB2 and MRSD– distributions assume a particularly rapid growth of the parton densities with decreasing x, see sect. 6. The MRS parametrizations were bound to fit the recent structure function data of the NMC collaboration which extend to $x = 0.008$ at $Q^2 = 4\ GeV^2$.

The H1 and ZEUS cross section measurements are consistent. Despite their limited statistical and systematic value both allow to rule out extreme assumptions on a very rapid growth or flattening of the structure functions towards $x \sim 10^{-4}$. H1 made a quantitative comparison presenting an integrated deep inelastic scattering cross section of $\sigma = (92 \pm 11(syst) \pm 12(stat))nb$. This value is compatible with both MRS distributions giving 88 nb (D0) and 128 nb (D–) but disfavours a large cross section as predicted by the MTB2 parametrization of 158 nb. The theoretical numbers and curves are lower by a few % if instead of a vanishing longitudinal structure function (both H1 and ZEUS set R=0, eqn. 6) one assumes the standard QCD expressions for F_L. The event numbers of the first data were too small for decisive measurements of the structure function $F_2(x, Q^2)$ or cross section shapes, i.e. the physics conclusions strongly rely on the normalization and overall efficiency calculations. A new level of accuracy is being reached with the ongoing analysis of the about 20 times more deep inelastic data taken in the autumn of 1992.

6. Small x Physics at HERA

The first data from HERA has shown us a glimpse of the newly accessible small x region in deep inelastic scattering. This region has been recognized to be of considerable theoretical interest [24] since new phenomena are predicted to onset at small x. Moreover, precise predictions for Z^o, $W^{\pm}$, $b\bar{b}$, Higgs ... production cross sections at future large hadron colliders, such as the LHC and SSC, depend critically on the knowledge of parton distributions in the range of very small $x \simeq 10^{-3} - 10^{-5}$.

Since the small x region is unexplored experimentally, extrapolations of presently proposed parton distributions in this range vary wildly. Evolution equa-

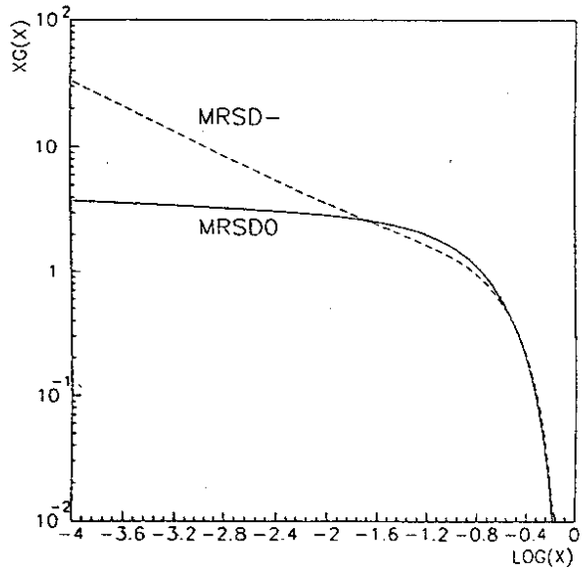

Figure 9: *Gluon distribution for the parametrizations MRSD0 and MRSD− for* $Q^2 = 5\ GeV^2$

tions in perturbative QCD predict a fast growth of the gluon density $xG(x)$ in the proton, for small x. The linear evolution equation particularly adapted to study the small x region is the Kuraev-Fadin-Lipatov equation [25], which predicts a characteristic $x^{-\lambda}$ behaviour of the gluon density at small x, with $\lambda \sim 0.5$. This has to be contrasted with the traditional expectations in the naive Regge-parton model where $xG(x) \sim x^{1-\alpha_{P(0)}}$, with the Pomeron intercept $\alpha_{P(0)} \simeq 1$, hence $xG(x) \sim$ constant. Fig. 9 shows the gluon distribution, $xG(x, Q^2)$, for the MRSD0 and MRSD− parton parametrizations [20], which include experimental information of the new NMC and CCFR data. The small x behaviour of the gluon density (at $Q_0^2 = 4\ GeV$) is assumed to be singular $x^{-0.5}$ for the MRSD− parametrization and constant for the MRSD0 parametrization.

At low x the sea quark distribution is driven by the gluon distribution, thus the $F_2(x, Q^2)$ evolution at small x will reflect the assumptions made on $xG(x, Q^2)$. For example, assuming an $x^{-0.5}$ behaviour of the gluon density results in a rapid growth of $F_2(x, Q^2)$. Since $F_2(x, Q^2) \sim \sigma_{tot}^{\gamma^*}$ a continuing increase would lead to an unphysical blowup of the cross section. Therefore, at very small x the rise of the gluon density must be damped by a new mechanism. A proposed scenario is that at small x the parton densities become so large that annihilation and recombination of parton pairs will start to compete with the parton decay processes taken into account in the standard evolution equations. Such "screening" or "shadowing" effects damp the fast increase of the parton density.

The emerging picture for the $F_2(x, Q^2)$ evolution at small x is shown in Fig. 10a where three regions A, B and C are distinguished. In the first region A, the evolution is described by the standard QCD evolution equations. In region B the onset of parton-parton recombination or annihilation sets in, but the x evolution can

be still described by improved evolution equations, such as the ones formulated by Gribov, Levin and Ryskin in 1983 [26]. Finally, in region C the density of partons becomes so large that they cannot be considered free any longer and non-perturbative confinement effects will start to play a rôle. Solid theoretical tools to study this region are unfortuantely not available yet.

Several theoretical estimates were presented for the border lines of these regions [27]. These depend critically on the assumptions on the shape of the gluon distribution at a small reference Q_0^2, say 5 GeV^2, and on the locality of the screening regions. One could assume that the large gluon density increase does not develop uniformly over the full transverse size of the proton, but is localized instead in small regions, so called "hot spots". Such a scenario results in large corrections to the standard evolution equations (strong screening), compared to the situation where the gluon density increase is spread uniformly over the proton (weak screening). In all, the theoretical expectation is that HERA will probe regions B and C if the gluon distribution shows the Lipatov $x^{-0.5}$ behaviour and the onset of screening is localized in hot spots. Region B is expected to be very narrow at HERA.

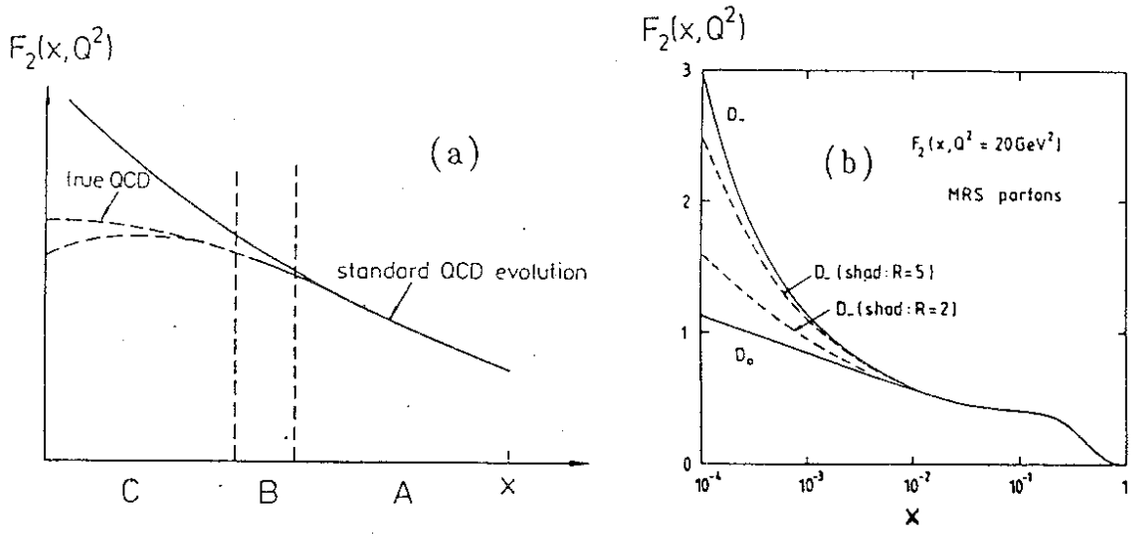

Figure 10: *a) Small-x behaviour of the structure function: standard QCD evolution versus "true QCD" evolution. Labels A, B and C denote the region of perturbative QCD, the transition region and the nonperturbative region, respectively. b) The structure function $F_2(x, Q^2)$ as function of x at $Q^2 = 20$ GeV^2. The solid line results from an F_2 without shadowing corrections, while the dashed lines correspond to the MRSD– prediction with weak (R_{shad}=5) and strong (R_{shad} =2) shadowing corrections (from [20]).*

It may turn out to be difficult to identify unambiguously the onset of a new regime from $F_2(x, Q^2)$ studies alone as it measures the parton density averaged over the full transverse size. Fig.10b shows F_2 for fixed Q^2, for singular and flat gluon density behaviour, with strong and weak screening. It turns out that it will be

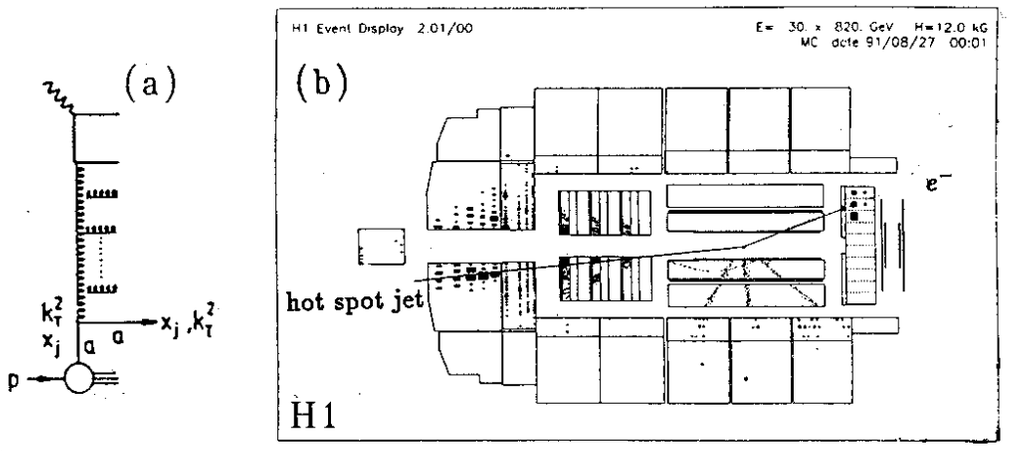

Figure 11: *a) Diagrammatic representation of a deep inelastic scattering event with an associated jet with momentum fraction x_j and virtuality k_T^2. b) A "hot spot" event generated by Monte Carlo generator. Kinematic variables are: $Q^2 = 75\ GeV^2$, $x = 0.005$, $x_j = 0.02$, $k_T^2 = 20\ GeV^2$.*

difficult to distinguish the strong screening and flat gluon behaviour predictions at HERA. For this purpose simultaneous evolution in Q^2 and x was studied in [28]. The difference between the results of the standard and improved evolution equations for the strong screening scenario will be at most 10-20% at the smallest values of x reachable at HERA.

Several alternative, dedicated measurements have been proposed to search for the presence of hot spot regions in the proton. One method, based on the idea of Mueller [29], is to measure the associated jet cross section as depicted in Fig.11a. For this measurement we determine the cross section of jets with a certain momentum fraction x_j (not to be confused with the Bjorken-x defined at the boson-quark vertex) and virtuality (transverse momentum squared) $k^2 = -k_T^2$. Cross section calculations for this process are given in [30] and deviations due to screening effects are expected to be large. The cross sections are sizeable, but for the interesting region where $x_j >> x$ the event topography is such that the associated jet is close to the beampipe (Fig. 11b), making this measurement an experimental challenge.

7. Summary and Prospects

More than 20 years after the discovery of the quark-parton substructure we are facing a new milestone in the physics of deep inelastic lepton nucleon scattering with the advent of the first electron-proton collider HERA at Hamburg. The successful operation of this collider including the detectors and their timely completion, can be considered as one of the major technical achievements of the high energy physics community. The very first data at modest luminosity have opened the experimental investigation of a new kinematic region: the region of small x, where parton densities are expected to be very large and effects predicted which

may change the established view on the quark-gluon interactions. Both the H1 and the ZEUS experiment have taken data right from the beginning of ep interactions, filtered out the very rare signal of deep inelastic scattering and were able to publish the first cross section measurement results in the same year. About 20 times more data are being analyzed which will allow to derive the first measurements of the structure function $F_2(x, Q^2)$ in the deep inelastic regime down to $x \sim 10^{-4}$. Further accumulation of high quality data will lead to the search for local parton density fluctuations (hot spots) and measurements of the longitudinal structure function which gives direct access to the behaviour of the gluon distribution at low x.

Acknowledgements

We would like to thank the organizers of the San Miniato Conference for inviting us to this traditional place. The results summarized here are due to the joint effort of may be as many as 1500 physicists and engineers. We are grateful to J.Feltesse, M.Leenen, Th.Naumann, S.Schlenstedt and P. Söding for critically reading the manuscript.

8. References

1. M. Breidenbach et al., *Phys.Rev.Lett.* **23** (1969) 935.
2. A rather comprehensive account of the first physics results from HERA has been published by G.Wolf, *DESY report* **92-190** (1992)
3. A.A.Sokolov and M.Ternov, *Dokl.Sov.Akad.Nauk* **8** (1964) 1203.
4. D.Barber et al., *DESY report* **92-136** (1992)
5. J.Buon and K.Steffen, *DESY report* **85-128** (1985)
6. B.Wiik, Contribution to the IEEE Particle Accelerator Conference, San Francisco, 1991, *DESY HERA report* **91-10** (1991);
   F.Degele, Contribution to the 3rd International Particle Accelerator Conference, Berlin, 1992, *DESY HERA report* **92-12** (1992);
   Contributions to the XVth International Conference on High Energy Accelerators, Hamburg, 1992, *DESY HERA report* **92-19** (1992);
   and references cited therein
7. H1 Collaboration, Technical Proposal, Hamburg 1986
8. ZEUS Collaboration, Technical Proposal, Hamburg 1986
9. H.Bethe and W.Heitler, *Proc.Roy.Soc.* **A146** (1934) 83.
10. T.Ahmed et al., H1 Collaboration, Total Photoproduction Cross Section Measurement at HERA Energies, *Phys.Lett.* **B299**, to appear
11. M.Derrick et al., ZEUS collaboration, *Phys.Lett.* **B293** (1992) 465.
12. T.Ahmed et al., H1 Collaboration, Observation of Deep Inelastic Scattering at Low x, *Phys.Lett.* **B299**, to appear

13. M.Derrick et al., ZEUS Collaboration, Initial Study of Deep Inelastic Scattering at HERA, submitted to *Phys.Lett.* **B**

14. S.Bentvelsen, P.Kooijman and J.Engelen, Proceedings of the Workshop "Physics at HERA", held at DESY, Oct. 1991, Hamburg 1992 Vol.1 p.23;
K.C.Hoeger, Proceedings of the Workshop "Physics at HERA", held at DESY, Oct. 1991, Hamburg 1992 Vol.1 p.43

15. A.Blondel and F.Jacquet, Proceedings of the Study of an *ep* Facility for Europe, ed. U.Amaldi, *DESY* **79/48** (1979) 391

16. J.Blümlein, *Phys.Lett.* **B271** (1991) 267;
A.Akhundov et al., Proceedings of the Workshop "Physics at HERA", held at DESY, Oct. 1991, Vol.3, p.1285

17. A. Kwiatkowski, H. Spiesberger, and H.-J. Möhring, *Comp.Phys.Commun.* **69** (1992) 155 and references therein.

18. G. Ingelman, "LEPTO 5.2", unpublished program manual;
H.Bengtsson, G.Ingelman, and T.Sjöstrand, *Nucl.Phys.* **B301** (1988) 554

19. L. Lönnblad, ARIADNE version 4.03, *Comp.Phys.Commun.* **71** (1992) 15 and references therein

20. A.D.Martin, W.J.Stirling, R.G.Roberts, *Durham preprint*, DTP-92-16 (1992).

21. S.Schlenstedt, private communication

22. A.Achundov and D.Yu.Bardin, private communication

23. J.Morfin and W.K.Tung, *Z.f.Phys.* **C52** (1991) 13

24. J.Bartels and J.Feltesse, Proceedings of the Workshop "Physics at HERA", held at DESY, Oct. 1991, Hamburg 1992 Vol.1 p. 133

25. E.A.Kuraev, L.N.Lipatov and V.S.Fadin, *Phys.Lett.* **60B** (1975) 50;
Zh.E.T.F **72** (1977) 377

26. L.V.Gribov, E.M.Levin and M.G.Ryskin, *Nucl.Phys.* **B188** (1981) 555;
Phys.Rep. **100** (1983)

27. J.Bartels and G.A.Schuler, Proceedings of the Workshop on LHC, *CERN report* **90-10** (1990) 865;
M.G.Ryskin and V.T.Kim *Sovj.J.Nucl.Phys.* **55** (1992) 623;

28. J.Bartels, J.Feltesse and K.Charchula, Proceedings of the Workshop "Physics at HERA", held at DESY, Oct. 1991, Hamburg (1992) Vol.1 193

29. A.H. Mueller, *Nucl.Phys.***B***(Proc.Suppl.)* **18C** (1990) 125

30. J.Bartels, A. De Roeck and M.Loewe, *Z.f.Phys.* **C54** (1992) 635;
W.K.Tung, *Phys.Lett.* **B278** (1992) 363;
J. Kwiecinski, A.D.Martin and P.J.Sutton, *Phys.Rev.* **D46** (1992) 921;
J. Kwiecinski, A.D.Martin and P.J.Sutton, *Phys.Lett.* **B287** (1992) 254